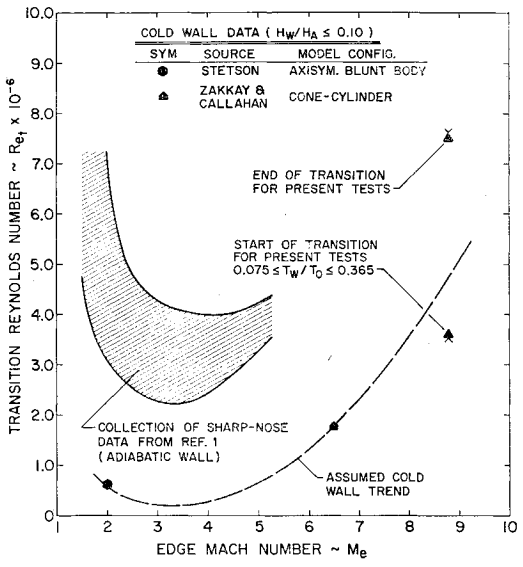

Fig. 3 Transition Reynolds number variation with local edge Mach number.

presented here with the compilation of data presented in Ref. 1 is given in Fig. 3, which depicts the variation of transition Reynolds number with local Mach number. The collection of data from Ref. 1 is for sharp-nose configurations having adiabatic-wall conditions. Cold-wall data of Stetson[6] and Zakkay,[7] also presented, form the basis of the assumed cold-wall trend depicted. The data obtained in the present investigation together with those of Refs. 6 and 7 corroborate the assumption that the transition Reynolds numbers increase with increasing edge Mach numbers.

Conclusions

On the basis of the data presented here, it can be concluded that transition reversal does not occur in the range of wall-to-stagnation temperature ratios of $0.075 \leq T_W/T_0 \leq 0.365$ and over the range of bluntnesses of $0.0 \leq r_N/r_B \leq 0.0572$ on a 5° semi-vertex-angle cone tested at a Mach number of 10. Of further interest are the significant effects of small amounts of nose bluntness on the observed transition Reynolds numbers, lengths of the transition regions, the insensitivity of transition Reynolds number to the variation of the wall-to-stagnation temperature ratio, and the apparent increase of transition Reynolds numbers with increasing edge Mach numbers.

References

[1] Savage, S. B. and Bendor, E. "Boundary layer transition at supersonic speeds," Republic Aviation Corp. Rept. RAC 1643 (July 1963).

[2] Sanator, R. J., Savage, S. B., DeCarlo, J. P., Torrillo, D. T., Casaccio, A., and Cousin, S. B., "Experimental and theoretical investigation of inlets for supersonic combustion ramjets," Air Force Flight Dynamics Lab. Rept. FDL TDR 64-119 (October 1964).

[3] Himka, T. and Luchuk, W., "Description of the Republic Aviation Corporation wind tunnel facilities," Republic Aviation Corp. Rept. 2380 (WT-TDR-64-102) (May 1964).

[4] Eckert, E. R. G., "Engineering relations for friction and heat transfer to surfaces in high velocity flow," J. Aerospace Sci. **22**, 585–587 (1955).

[5] Moekel, W. E., "Some effects of bluntness on boundary-layer transition and heat transfer at supersonic speeds," NASA Rept. 1312 (1957).

[6] Stetson, K. F., "Boundary-layer transition on blunt bodies with highly cooled boundary layers," J. Aerospace Sci. **27**, 81–91 (1960).

[7] Zakkay, V. and Callhan, C. I., "Laminar, transitional, and turbulent heat-transfer to a cone-cylinder-flare body at Mach 8.0," J. Aerospace Sci. **29**, 1403–1413 (1962).

Nuclear Heating and Propellant Stratification

EDWARD E. DUKE*
Aerojet-General Corporation, Sacramento, Calif.

Introduction

IN order to obtain maximum vehicle performance for a nuclear system employing liquid hydrogen [$H_2(l)$], the vehicle must be designed to obtain optimized propellant utilization while minimizing system weight. A major problem encountered in this endeavor is caused by propellant heating.

Propellant heating has the undesirable effect of raising the temperature of the liquid to a value that is no longer acceptable for adequate main feed pump operation. To insure proper propellant utilization and to prevent pump cavitation, the propellant temperature distribution during pump operation must be accurately predicted.

The determination of the temperature history of the propellant leaving a nuclear vehicle tank involves many influencing variables. The problem is that of determining the flow field in the tank and the effect of mixing caused by density variations within the liquid. Recent experimental evidence indicates that bulk heating is an important effect in small tanks since the stratified layer in the conical section apparently mixes quite profusely.[1] For larger tanks, however, nuclear heating may contribute as much as 5–10% to the total increased heat content of a stratified layer.[2, 3] Comparative information is based on severely simplified analytical models and inadequate test results.[2,4] This note suggests one method of analyzing stratification caused by nuclear bottom heating in large tanks and compares the results to bulk and inversion point calculations.

The system analyzed (see Fig. 1) is a closed cylindrical-cone-bottomed tank accelerating along its longitudinal axis and filled with liquid to some height. This liquid is subjected to a time- and position-varying group of heat fluxes, q_ℓ = ullage, q = wall, and q_{up} = nuclear. The ullage temperature is above the saturation pressure corresponding to the liquid surface temperature. Wall-heat flux to the ullage is considered to be negligible, the ullage pressure being maintained by automatic control valving.

An approximate stratification solution is obtained by assuming a temperature profile in the stratified layer, the growth of which is determined by the evaluation of each of the three independent heat fluxes. The calculations follow those outlined in Ref. 5 with the inclusion of q_{up} in q.

Bottom Gravitational Convection (q_{up})

The turbulent gravitational convection mechanism appears to be one means of describing the upward flow of liquid from a tank heated by nuclear deposition within the bottom bulk. For a unified treatment of all kinds of convection which can take place in a gravitational field, the excess temperature must be replaced by the equivalent deficiency of density under that of the surroundings. But the sole relevant effect of a deficiency of density is to create a buoyancy force. The strength of a source of heat in a region of fluid is measured by the total heat output to the neighboring fluid in unit time. Similarly, the strength of a source of buoyancy is the total rate of release of buoyance to the nearby fluid. In the present analysis, each segment of tank bottom is viewed as a possible source of upward mass and energy flow. Boundary segment movement alters the conditions within neighboring segments. Through a balancing and summation routine, the warm mass that moves upward and joins the side-wall boundary

Received November 2, 1964.

* Senior Engineer, Rocket Engine Operations-Nuclear, Advanced Concepts. Member AIAA.

layer is calculated. Equations pertinent to individual internal heated segments for flux of buoyancy per second F_0, gravity variable G, and density gradient $d\rho_1/dz$ are

$$\frac{\pi}{2f}\left\{\left[g_z\left(\frac{\rho_1-\rho}{\rho_1}\right)\frac{6}{5}\gamma z^{5/3}\right]^{3/2}\left(\frac{9}{10}\gamma\right)^{1/2}\right\}=F_0 \qquad (1)$$

where ρ_1, ρ, and γ are reference density, segment density, and entrainment constant, respectively, whereas f is a transformation value that varies with segment height z, and

$$G=g_z/\rho_1\, d\rho_1/dz \qquad \text{where} \qquad d\rho_1/dz=(\rho_1-\rho)/z \qquad (2)$$

The velocity of the segment mass is derived from the boundary conditions set at the source and the physical conditions of F_0 and G, these determining the scale of motion[6]

$$V_{\text{seg up}}=1.158\gamma^{-1/2}F_0^{1/4}G^{1/8}(v^2/w) \qquad (3)$$

where v^2/w is a transformation varying with z. Experimentally, γ, f, v, and w have never been evaluated in $H_2(l)$. Data from Ref. 6 are thus used most appropriately at this time. It follows therefore that the heat rate, if upward, as determined by Eqs. (1) and (2) and V_{down}, is then

$$q_{\text{up}}=(V_{\text{up}}-V_{\text{down}})\rho_1(T_{\text{seg}_{\text{new}}}-T_{\text{seg}_{\text{old}}})C_P \qquad (4)$$

With propellant flow in the downward direction, Eq. (4) will hold only if $V_{\text{up}} > V_{\text{down}}$. In order for this relationship to suffice, it can be seen from the equations that $F_0[f(\text{heat in})]$ must be large, V_{down} small, or a combination of the two. For a tank shape as shown in Fig. 1 and nuclear heat distribution as discussed in Ref. 4 (decreasing with tank height but with higher rates at walls than in interior), it can be expected that upward flow can initiate most easily along the slanted wall at some height z where wall and nuclear heat flux are large and downward velocity is small. This "initiation" point can be compared to Vliet's "inversion" point concept based on differing arguments.

Inversion Point Convection

The location of the inversion point is determined by the shape of the bottom, the liquid out-flow rate, and the heating and acceleration environments. Above the inversion point, the dominant buoyant forces cause the boundary layer to flow upward, and below the inversion point, the dominant pressure forces cause the boundary layer to flow downward. The temperature of all adjacent layers above and at the inversion point is examined for negative temperature gradients, and these temperatures are equalized with energy being conserved, each layer retaining its original mass. Vliet's assumption is that unstable inversion cannot be permitted, and upward flow within the boundary layer must take place even though the present concept admits the existence of the inversion (with heat from the wall to segments beyond) and utilizes this inversion to drive the heated liquid upward. Photographs have been unsatisfactory in determining which, if any, mechanism persists.[5,7] The inversion point equation is

$$R_{\substack{\text{tank radius}\\ \text{at inversion}}}=0.4\left(\frac{kP_r^{0.4}}{\beta\nu^{3/4}}\right)^{0.148}\left(\frac{1}{\rho}\right)^{0.407}w^{0.407}\times\left(\frac{1}{g^*\,q_{\text{wall}}}\right)^{0.148}\left\{\frac{(dR/dx)}{[1-(dz/dx)]^{0.407}\,(dz/dx)^{0.148}}\right\} \qquad (5)$$

where w and x are mass flow rate and slant height, respectively, and g^* is the number of standard gravities.

Comparisons

References 2 and 4 describe an experimental arrangement designed to simulate the radiation source and the $H_2(l)$ propellant-tank geometry of a typical nuclear rocket system. The Aerospace Systems Test (AST) Reactor was utilized as the source of nuclear radiation with a 125-gal $H_2(l)$ tank in use. Experimental run 16A-110[1] operating at 1.065-Mw thermal power with an average flow rate of 10.4 gal/min is investigated analytically for inversion and initiation points. Heat generation along x from the tank bottom to the top of the cone experimentally ranged from 300–22 Btu/ft^3-hr, whereas wall heat flux was calculated as 12.25 Btu/hr-ft^2. These data were used to evaluate both the initiation point and the inversion point, the results being: 1) initiation point [Eqs. (1–4)] from bottom = 0.582 ft, 2) inversion point [Eq. (5)] from bottom = 0.390 ft, and 3) depth of tank bottom cone = 1.630 ft. The comparison is good when differences of approach and uncertainty in empirical constants are considered. No experimental data are as yet available for noteworthy comparison or verification.

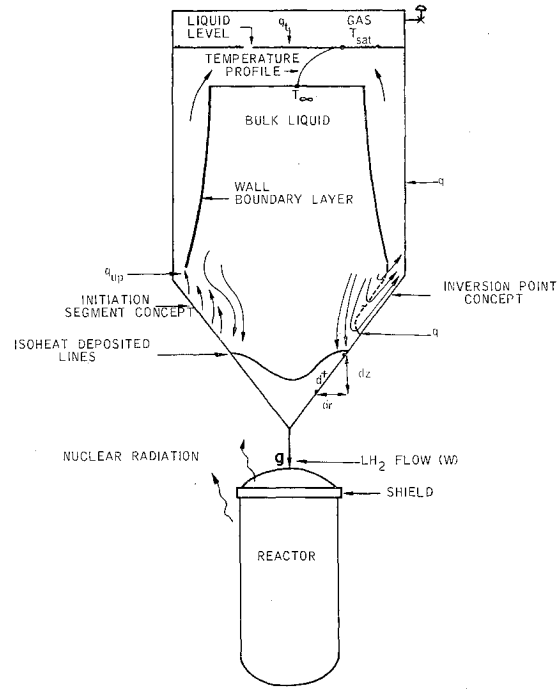

Fig. 1 Stratification flow model.

Calculation of the stratified layer in the cylindrical tank portion for two models by the method described in the Introduction (run 16A-110) has been made and the results are shown in Fig. 2. The stratified-layer temperature distribution was evaluated first with bulk bottom mixing and then with the more realistic nuclear bottom heating with segment initiation upward flow. A comparison of the results shows a significant difference, but the exact nature of the difference depends upon the evaluation of the empirical constants previously discussed.

Conclusions

An approximate analysis of the transient stratification of a closed fluid container that is subject to wall, ullage, and

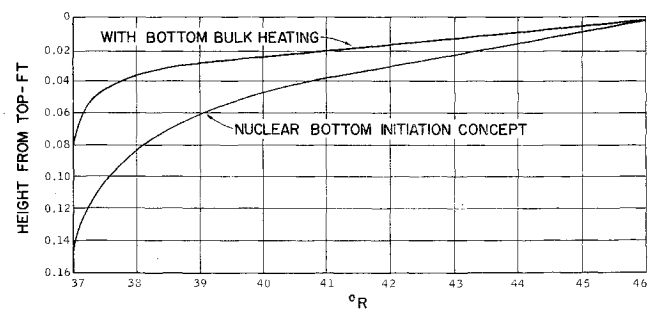

Fig. 2 Comparison of bottom bulk and nuclear initiation stratification 85 sec after run start.

nuclear heating has been discussed. The results rely upon the assumptions of continuous temperature profile build-up in the stratified layer, nuclear heating effects described by a gravitational-free convection mechanism, and the separability of the various heat-transfer sources. The method of gravitational-free convection (initiation concept) has been proposed as an alternate solution to inversion point boundary-layer flow. The preliminary comparison is good. In addition, temperature stratification using nuclear-heated, gravitational-free flow indicates that the higher discharge temperatures from such a system for large tanks may be approximated by the method proposed. However, continued conscientious efforts, experimentally and analytically, in the development of the stratified growth, radiation-excitation storage, and turbulent nuclear heat mechanisms are needed.

References

[1] Hehs, W. H., personal communications, General Dynamics/Fort Worth NARF (February–May 1964); partially presented in Ref. 2.

[2] Hehs, W. A. and Miller, G. E., "Nuclear radiation heating in liquid hydrogen," General Dynamics/Fort Worth Rept. FZK 186, Vols. 1 and 2, NASA CR-54078 (June 1964).

[3] Connolley, D. J., personal communication, Advanced Development Evaluation Div., NASA Lewis Research Center (November 1963).

[4] Hehs, W. A. and Miller, G. E., "Measured and calculated nuclear radiation distributions in liquid hydrogen," General Dynamics/Fort Worth Rept. FZK-182, NASA CR-54003 (March 1964).

[5] Tatom, J. W., Brown, W. H., Knight, L. H., and Coxe, E. F., "Analysis of thermal stratification of LH_2 in rocket propellant tanks," Lockheed-Georgia Paper E-3 (1963); also Cryogenic Engineering Conference, Boulder, Colo., Paper E3 (August 1963).

[6] Morton, B. R., Taylor, G., and Turner, J. S., "Turbulent gravitational convection from maintained and instantaneous sources," Proc. Roy. Soc. (London) **A234**, 1–123 (January 1956).

[7] Vliet, G., "Stratified layer flow model—a numerical approach to temperature stratification in liquids contained in heated vessels," Lockheed Missiles and Space Co., TR-8-30-63-4 (November 1963).

Stagnation-Point Velocity Distribution for a Compressible Fluid

ROBERT A. GRAFF*

Union Carbide Research Institute, Tarrytown, N. Y.

Nomenclature†

a, b, c_n, d_n = const
I_0 = zero-order modified Bessel function of the first kind
K_0 = zero-order modified Bessel function of the second kind
M = Mach number at reference point
r = radial coordinate
R_n = finite cosine transform defined by Eqs. (9–11)
V_r = radial velocity
V_z = axial velocity
z = axial coordinate
α_n = defined by Eq. (25)
β_n = defined by Eq. (26)
γ = ratio of specific heat at constant pressure to that at constant volume
ϕ = velocity potential‡
ϕ_0, ϕ_1, ϕ_2 = zero, first, second perturbation to the velocity potential [Eq. (5)]‡

Received November 2, 1964. This work was supported by the Advanced Research Projects Agency Propellant Chemistry Office and was monitored by the Army Missile Command under Contract No. DA-30-069-ORD-2787.

* Consultant; also Assistant Professor, the City University of New York.

† Cylindrical coordinates are used with the origin at the stagnation point and the z axis normal to the surface. An upstream point on the z axis at which the velocity is known is taken as a reference point. Coordinates r and z are normalized on the distance from the reference point to the stagnation point. Velocities V_r and V_z are normalized on the fluid velocity at the reference point.

POTENTIAL flow solutions are prerequisite to boundary-layer calculations. For the case of a fluid stream impinging on a wall at right angles and flowing away radially, no velocity distribution, taking into account compressibility effects, appears to be available in the literature. It is the purpose of this note to present a solution for subsonic flows. The result, found by carrying the Rayleigh-Janzen method[1] to the second perturbation, is

$$V_r = \frac{r}{2} + M^2\left(\frac{r^2}{16} - \frac{1}{3}\right)\frac{r}{2} + M^4\left[\left(\gamma + \frac{3}{2}\right)\frac{r^4}{64} - \frac{2\gamma+1}{16}r^2 + \frac{\gamma-1}{5} + \frac{\gamma-1}{8}\left(-\frac{7}{30} + z^2 - \frac{z^4}{2}\right)\right]\frac{r}{6} \quad (1)$$

$$V_z = -z + M^2(1-z^2)\frac{z}{3} + M^4\left[\frac{\gamma-1}{2}(1-z^2)r^2 - (23\gamma+57)\frac{z^4}{10} + (11\gamma+13)\frac{z^2}{3} - \frac{41}{30}(\gamma-1)\right]\frac{z}{24} \quad (2)$$

This was obtained by the following procedure.

From the hydrodynamic equations describing potential flow an expression may be found for the velocity potential ϕ in the form [Ref. 1, p. 291, Eq. (9.46)]

$$\frac{1}{r}(r\phi_r)_r + \phi_{zz} = \frac{\phi_r^2\phi_{rr} + \phi_z^2\phi_{zz} + 2\phi_r\phi_z\phi_{rz}}{(1/M^2) + [(\gamma-1)/2][1 - (\phi_r^2 + \phi_z^2)]} \quad (3)$$

with boundary conditions

$$\phi_z = -1 \text{ at } z = 1$$
$$\phi_z = 0 \text{ at } z = 0 \quad (4)$$

and the requirements that ϕ_r be finite at $r = 0$ and well behaved for large values of r. Following the Rayleigh-Janzen method, we take ϕ to be a power series in M^2

$$\phi_0 + M^2\phi_1 + M^4\phi_2 + \ldots \quad (5)$$

By substituting Eq. (5) into Eq. (3), and equating coefficients of like powers of M,

$$(1/r)(r\phi_{0r})_r + \phi_{0zz} = 0 \quad (6)$$

$$(1/r)(r\phi_{1r})_r + \phi_{1zz} = \phi_{0r}^2\phi_{0rr} + \phi_{0z}^2\phi_{0zz} + 2\phi_{0r}\phi_{0z}\phi_{0rz} \quad (7)$$

$$(1/r)(r\phi_{2r})_r + \phi_{2zz} = 2\phi_{0r}\phi_{1r}\phi_{0rr} + \phi_{0r}^2\phi_{1rr} + 2\phi_{0z}\phi_{1z}\phi_{0zz} + \phi_{0z}^2\phi_{1zz} + 2[(\phi_{0r}\phi_{1z} + \phi_{0z}\phi_{1r})\phi_{0rz} + \phi_{0r}\phi_{0z}\phi_{1rz}] - [(\gamma-1)/2][(1/r)(r\phi_{1r})_r + \phi_{1zz}][1 - (\phi_{0r}^2 + \phi_{0z}^2)] \quad (8)$$

These equations are solved seriatim by application of the finite cosine transform on z

$$F(r,z) = \sum_{n=0}^{\infty} R_n(r)\cos(n\pi z) \quad (9)$$

$$R_0(r) = \int_0^1 F(r,z)dz \quad (10)$$

‡ Subscripts r and z on ϕ, ϕ_0, ϕ_1, ϕ_2 are used to indicate differentiation.